Endocrine (2019) 64:130–138
https://doi.org/10.1007/s12020-019-01842-y

ORIGINAL ARTICLE

Mutational profile of papillary thyroid microcarcinoma with extensive lymph node metastasis

Min Ji Jeon[1] · Sung Min Chun[2,3] · Ji-Young Lee[3] · Kyeong Woon Choi[4] · Deokhoon Kim[3] · Tae Yong Kim[1] · Se Jin Jang[2] · Won Bae Kim[1] · Young Kee Shong[1] · Dong Eun Song[2] · Won Gu Kim[1]

Received: 15 October 2018 / Accepted: 4 January 2019 / Published online: 15 January 2019

Abstract

Purpose Papillary thyroid microcarcinoma (PTMC) has excellent outcomes, but extensive lymph node (LN) metastasis can be associated with fatal outcomes. We evaluated the mutational profiles of primary tumors and their metastatic LNs of PTMCs with extensive lateral cervical LN metastases.

Methods Formalin-fixed, paraffin-embedded archival samples from 16 sets of normal thyroid tissue, the primary PTMC, and the largest metastatic LN were used for targeted sequencing.

Results A total of seven somatic variants were confirmed in the PTMCs compared to the normal tissue. The *BRAF*^{V600E} mutation was the most common and seen in 12 primary tumors (75%) and 11 metastatic LNs (69%). A nonsense mutation in *AR* and an in-frame deletion in *ACVR2A* were detected in one primary tumor and its metastatic LN (6%). Missense mutations in *KMT2A*, *RAF1*, and *ROS1* were detected in one primary tumor (3%). A frameshift deletion mutation in *JAK2* was detected in a metastatic LN (3%). In PTMCs without the *BRAF* mutation, an *ALK* and *RET* rearrangement (one PTMC and its metastatic LN, 6%) was detected. In one patient, the *BRAF* mutation was detected in the primary tumor, but only a *RET* rearrangement was detected in its metastatic LN. No mutations were detected in two patients.

Conclusion The mutational frequency of PTMCs was really low, even in those with extensive LN metastasis. The mutational status of the primary tumor and its metastatic LNs were not significantly different, and this suggests a minor role for genetic alterations in the process of LN metastasis in PTMC.

Keywords Papillary thyroid microcarcinoma · DNA mutational analysis · High-throughput nucleotide sequencing · Translational research

Introduction

Papillary thyroid microcarcinoma (PTMC), which is papillary thyroid carcinoma (PTC) that is ≤1 cm at the longest diameter, is the most indolent subtype of thyroid cancer [1, 2]. In our previous study, the disease-specific mortality from PTMC was only 0.05% during the median 8 years of follow-up, and distant metastasis was detected in 0.1% of PTMC patients. As distant metastasis was closely related to

These authors contributed equally: Min Ji Jeon, Sung Min Chun

Supplementary information The online version of this article (https://doi.org/10.1007/s12020-019-01842-y) contains supplementary material, which is available to authorized users.

✉ Dong Eun Song
desong@amc.seoul.kr

✉ Won Gu Kim
wongukim@amc.seoul.kr

[1] Department of Internal Medicine, Asan Medical Center, University of Ulsan College of Medicine, Seoul 05505, Korea

[2] Department of Pathology, Asan Medical Center, University of Ulsan College of Medicine, Seoul 05505, Korea

[3] Center for Cancer Genome Discovery, Asan Institute for Life Science, Asan Medical Center, University of Ulsan College of Medicine, Seoul 05505, Korea

[4] Asan Medical Institute of Convergence Science and Technology, Asan Medical Center, University of Ulsan College of Medicine, Seoul 05505, Korea

the disease-specific mortality, we evaluated the risk factors for distant metastasis of PTMC. We found that extensive lymph node (LN) metastasis, a lateral cervical LN metastasis with an extranodal extension or an aggressive pathologic subtype of metastatic LNs, is associated with fatal, distant metastasis in PTMC [3]. However, the mutational profile of these tumors was not evaluated in that study, and little is known about the differences in the mutational profile of primary thyroid cancer and its metastatic thyroid cancers.

BRAF is the most studied gene for PTMC, and the *BRAF* V600E mutation is the most common [4]. In a recent meta-analysis, the *BRAF* V600E mutation was detected in about 50% of PTMCs and was associated with aggressive clinicopathological characteristics, such as tumor multifocality, extrathyroidal extension, LN metastases, and advanced stage [5]. A telomerase reverse transcriptase (TERT) promoter mutation has also been reported in PTMCs, but has not been associated with unfavorable outcomes such as persistent/recurrent disease [6].

As the pathological change was significant in the metastatic LN of PTMC with distant metastasis compared to the primary tumor in our previous study, we hypothesized that primary PTMC and its metastatic LN might also be genetically different, and the difference in the mutational profile might be a surrogate marker for the prediction of distant metastasis of PTMC. In the present study, we aimed to evaluate the mutational profiles of PTMCs with extensive LN metastasis by targeted next-generation sequencing (NGS) and to investigate the differences in the mutational profile between the primary PTMC and its metastatic LN. A comprehensive evaluation of the mutational profile of PTMCs is important to understand the sequence of cancer progression and the metastatic cascade.

Materials and methods

Patients and tissue samples

After obtaining informed consent, we prospectively enrolled 14 PTMC patients with lateral cervical LN metastasis at the time of initial operation between 2011 and 2016, at the Asan Medical Center, Seoul, Korea. One patient who died of PTMC, and one patient who died of another malignancy, was also enrolled without informed consent. Therefore, a total of 16 PTMC patients were included in this study. Three of them also had distant metastases. Formalin-fixed, paraffin-embedded (FFPE) archival samples were collected from the primary tumor, the largest metastatic LNs, and matched normal tissues. All of these specimens were reviewed by an experienced endocrinology pathologist (D. E.S), and the pathologist selected adequate tissue blocks for the isolation of DNA. In patients with multifocal PTMCs, we selected the dominant tumor with the largest diameter. This study was approved by the Institutional Review Board of the Asan Medical Center, Seoul, Korea.

DNA extraction

After review of the matched hematoxylin/eosin-stained slides from each FFPE tissue section, 2–5 6-μm-thick slices from each specimen were used for the extraction of genomic DNA, depending on the sample size and tumor cellularity. After treatment with xylene and ethanol for de-paraffinization, genomic DNA was isolated using the NEXprep FFPE Tissue kit (#NexK-9000; Geneslabs, Korea), according to the manufacturer's protocol. Briefly, tissue pellets were lysed completely by incubation with proteinase K in the Lysis buffer overnight at 56 °C, followed by an additional incubation for 3 min with magnetic beads and Solution A at 37 °C. After incubation for 5 min on a magnetic stand, the supernatants were removed and washed three times with ethanol. After air-drying the beads for 5 min, DNA was eluted in 50 μL of nuclease-free water and quantified using a Qubit™ dsDNA HS Assay kit (Thermo Fisher Scientific, MA, USA) [7].

Targeted NGS

Targeted NGS was performed using the MiSeq platform (Illumina, San Diego, CA, USA) with OncoPanel AMC version 3 (OP_AMCv3) targeting a total of 382 genes, including the entire exons of 199 genes, 184 hot spots, and the partial introns of 8 genes often rearranged in cancer (Supplementary Table 1). Two hundred nanograms of gDNA were fragmented by sonication (Covaris Inc., Woburn, MA, USA) to an average size of 250 bp, followed by size selection using Agencourt AMPure XP beads (Beckman Coulter, High Wycombe, UK). A DNA library was prepared by sequential reactions of end repair, A-tailing, and ligation with a TruSeq adaptor, using a SureSelectXT Reagent kit (Agilent Technologies, Santa Clara, CA, USA). Each library was addressed with sample-specific barcodes of 6 bp and quantified using Qubit. Eight libraries were pooled to a total of 750 ng for hybrid capture using an Agilent SureSelectXT custom kit (OP_AMCv3 RNA bait; Agilent Technologies). The concentration of the enriched target was measured by quantitative PCR (Kapa Biosystems, Woburn, MA, USA), and the sample was loaded on the MiSeq platform or paired-end sequencing.

Bioinformatics analysis

Sequenced reads were aligned to the human reference genome (NCBI build 37) with the Burrows-Wheeler Aligner (0.5.9) [8] with the default options. De-multiplexing was

performed with MarkDuplicates of the Picard package to remove PCR duplicates (available at http://broadinstitute.github.io/picard). De-duplicated reads were re-aligned at known indel positions with the GATK IndelRealigner tool [9]. The base quality was recalibrated using the GATK TableRecalibration tool. Somatic single-nucleotide variants and short indels were detected with the matched normal, using Mutect (1.1.6) and the SomaticIndelocator tool in GATK [10]. Common and germline variants from the somatic variant candidates were filtered out with the common dbSNP (build 141; found in >1% of samples), Exome Aggregation Consortium (ExAC; r0.3.1, threshold frequency 0.001), Korean Reference Genome database (KRGDB), and an in-house panel of normal. Final somatic variants were annotated using the Variant Effect Predictor (version 79) and were then converted to the maf file format using vcf2maf (https://github.com/mskcc/vcf2maf). False-positive variants were manually curated using the Integrative Genomics Viewer (IGV). Minimum depth for detected alteration was 5× in our study. For the analysis of structural variations, copy number variation (CNV) and rearrangement were evaluated using the CNVkit [11] and BreaKmer [12] algorithms, respectively. After analysis of the CNV for primary tumor and metastatic LN against the matched normal, GISTIC algorithm was applied to the segmented files (CNS) for identification of significant focal and arm level amplifications and deletions [13]. The GISTIC *q*-value cutoff was set at 0.25 by the software's instruction. Candidates for germline mutations or false positives for rearrangement alterations by BreaKmer were filtered out with an in-house panel of normals and by manual review.

Results

Baseline characteristics of patients with PTMC

Table 1 presents the baseline characteristics of the PTMC patients included in this study. The median age of the patients was 49 years (interquartile range [IQR] 40–55), and 88% of the patients were females. The median primary tumor size was 0.9 cm (IQR 0.8–1.0), and 70% had microscopic extrathyroidal extensions of the tumor. All of these patients had lateral cervical LN metastasis (N1b disease by the 8th TNM staging system [14]). The median number of metastatic LNs was 11 (IQR 7–16) and the maximal size of the metastatic LNs was 1.4 cm (IQR 1.1–1.9). Extranodal extension of metastatic foci from the metastatic LNs was also detected in eight patients (50%). Three patients had synchronous distant metastasis, and one died of PTMC. Except for the patients with synchronous distant metastasis, one patient had locoregional structural recurrence in the lateral cervical area during follow-up.

Table 1 Baseline characteristics of 16 papillary thyroid microcarcinoma patients

Characteristics	*N* (%)	Median (IQR)
Age (years)		49 (40–54)
≥55	4 (25)	
Sex		
Male	2 (13)	
Female	14 (88)	
Size of primary tumor (cm)		0.9 (0.8–1.0)
Extrathyroidal extension		
No	5 (31)	
Microscopic	11 (69)	
Multifocality		
No	7 (44)	
Yes	9 (56)	
Cervical LN metastasis		
N1b	16 (100)	
No. of metastatic LNs		11 (7–16)
Maximal size of metastatic LNs		1.4 (1.1–1.8)
Presence of extranodal extension	8 (50)	
Distant metastasis		
M1 (Synchronous)	3 (19)	
Structural persistent/recurrent disease	1 (8)	
Locoregional	1 (8)	

Categorical variables are presented as numbers with percentages.

Continuous variables are presented as medians with interquartile ranges (IQR)

Significantly mutated genes in PTMCs

We performed targeted sequencing of 16 matched primary tumors, metastatic LNs, and normal thyroid tissue sets. After excluding germline mutations by comparing the sequencing results of the PTMCs or metastatic LNs with those of the matched normal tissues, we detected nine significantly mutated genes in the primary tumors or the metastatic LNs of PTMC (Fig. 1).

Among the seven somatic variants detected, the *BRAF* V600E mutation was the most common and was observed in 23 samples (72%) including 12 primary PTMCs (75%) and 11 metastatic LNs (69%). In one patient, a nonsense mutation of the androgen receptor (*AR)* and an in-frame deletion of the activin receptor 2A (*ACVR2A)* were detected in a primary PTMC with its LN (6.3%), respectively. The locations of the mutations in the *BRAF*, *ACVR2A*, and *AR* genes, which were frequently mutated genes in PTMCs and their metastatic LNs, are shown in lollipop plots (Fig. 2). In three separate primary PTMCs, missense mutations in *KMT2A*, *RAF1*, and *ROS1* were detected (3.1%). A frameshift deletion mutation in *JAK2* was detected in a metastatic LN (3.1%).

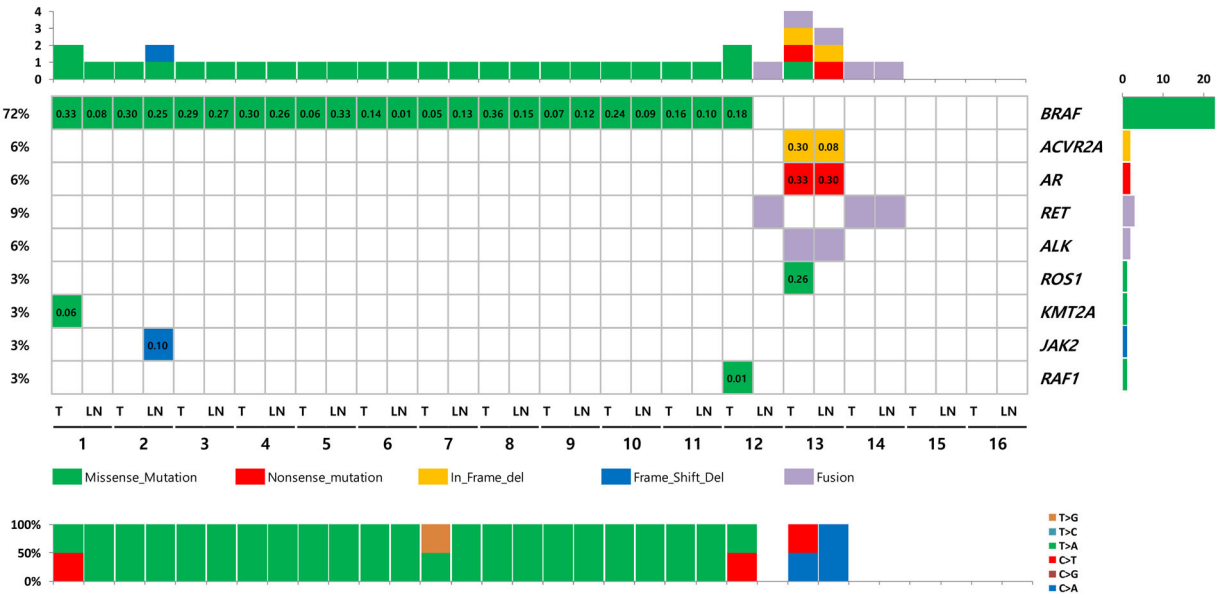

Fig. 1 Mutations in papillary thyroid microcarcinoma (PTMC) and its metastatic lymph node (LN), detected by targeted sequencing. Pairs of primary PTMC tumor and metastatic LN samples are arranged from left to right. The type of mutation is annotated for each sample by color with variant allele frequency value. The mutational frequencies for each mutated gene are plotted in the right panel. The mutation number is presented in the top panel. The types of base-pair substitutions of the somatic mutations are displayed in the bottom panel

In tumors without a *BRAF* mutation, we also found a *RET* intergenic rearrangement and *ALK/STRN* rearrangement in one PTMC with its metastatic LN (6.3%). In one patient, the *BRAF* mutation was detected in the primary tumor but only a *CCDC6/RET* rearrangement was detected in a metastatic LN (3.1%) (Fig. 1).

In total, the mean number of mutations per sample was 1.2 (range, 0–4) in primary tumors and 1.1 (range 0–3) in metastatic LNs. We could not find any mutations in two patients (Patients 15 and 16).

Pathological characteristics of PTMC with *ALK* rearrangement

The mutational frequency was especially high in one patient (Patient 13) with *ALK* rearrangement and we evaluated detailed pathological characteristics of this tumor. Tumor cells showed solid growth pattern with abundant cytoplasm, plasma cell infiltration, and metastatic tumor cells showed wide variation of nuclei size with occasionally observed prominent nucleoli (Fig. 3).

Mutational characteristics of PTMCs with distant metastasis or recurrence

All four PTMC patients with distant metastasis (Patients 1–3) or recurrent disease (Patient 9) had the *BRAF* V600E mutation. Patient 1 had the solid variant of PTMC with metastatic LNs showing anaplastic change and died of PTMC. Primary tumor had the *BRAF* and *KMT2D* mutation and its metastatic LN only had the *BRAF* mutation. Patient 2 had the classical variant of PTMC and showed diffuse lung metastasis. Lung metastasis was controlled after high-dose radioactive iodine treatment. The *BRAF* mutation was detected in the primary tumor. Its metastatic LN had the *BRAF* and *JAK2* mutation. Patient 3, who had the classical variant of PTMC with lung metastasis, and Patient 9, who had recurrent disease, had only the *BRAF* mutation.

Significant copy number variations in PTMC

We additionally performed a GISTIC2 analysis to detect significant focal CNVs, which yielded seven amplified and nine deleted regions (q-value <0.25; Fig. 4; Supplementary Tables 2 and 3). The most common focal deletion region was 9q34.12, containing *ABL1*, which has been reported as a recurrently deleted gene in PTC [15]. The most frequent focal amplified region was 5q13.2, which has not been reported previously.

Discussion

In this study, we performed targeted NGS of PTMC with its metastatic LN. All PTMCs analyzed in this study had extensive LN metastasis, and the median number and size of the metastatic LNs were 11 and 1.4 cm, respectively. Extranodal extension of metastatic foci from the metastatic LNs was also detected in 50% of patients. Furthermore, three patients had distant metastasis from PTMC, and one of

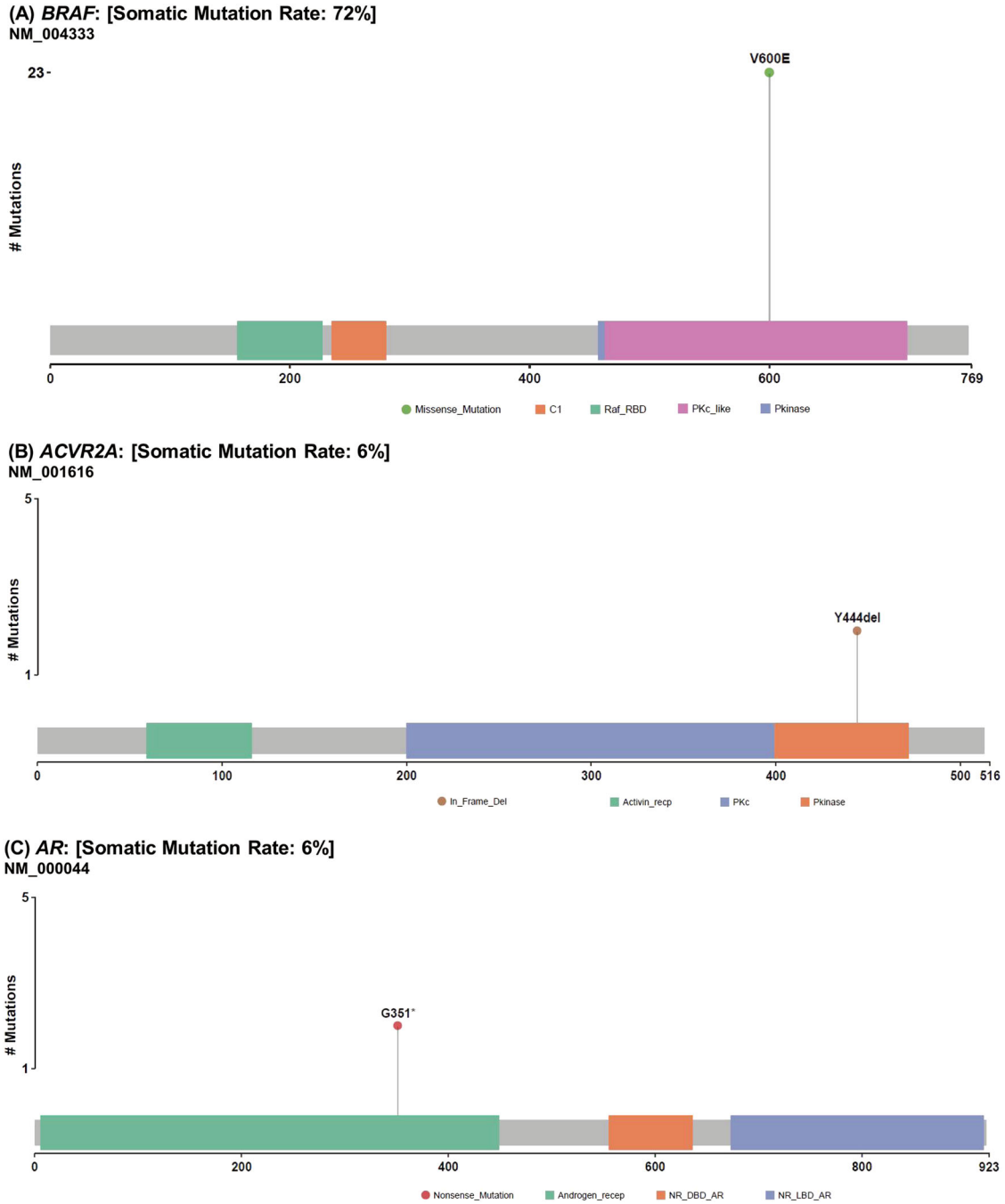

Fig. 2 Lollipop plots of frequently mutated genes in papillary thyroid microcarcinoma and its metastatic lymph node. **a** *BRAF* gene, **b** *ACVR2A* gene, and **c** *AR* gene. A position with a mutation is denoted by a circle, and the length of the line represents the number of mutations detected at the position. Colored boxes show the specific functional domains. **a** *BRAF* gene. RBD Ras-binding domain, PKinase-Tyr protein tyrosine kinase. **b** *ACVR2A* gene Activin_recp activin receptor domain, PK protein kinase. **c** *AR* gene Androgen_recep androgen receptor, NR_DBD_AR DNA-binding domain of the nuclear receptor of AR, NR_LBD_AR ligand-binding domain of the nuclear receptor of AR

them died of PTMC. Even in PTMCs with aggressive characteristics, the mutational frequency was really low, and the mean number of mutations per sample was only 1.1 (range, 0–4) [16].

The mutational status of the primary tumors and their metastatic LNs was not significantly different. In general, the mutational frequency did not differ. A frameshift deletion mutation in *JAK2* was only detected in the metastatic LNs, but missense mutations in *KMT2A*, *RAF1*, and *ROS1* were detected in only primary PTMCs. Our finding is consistent with a previous study that reported that the concordance of the genotype between primary tumors and

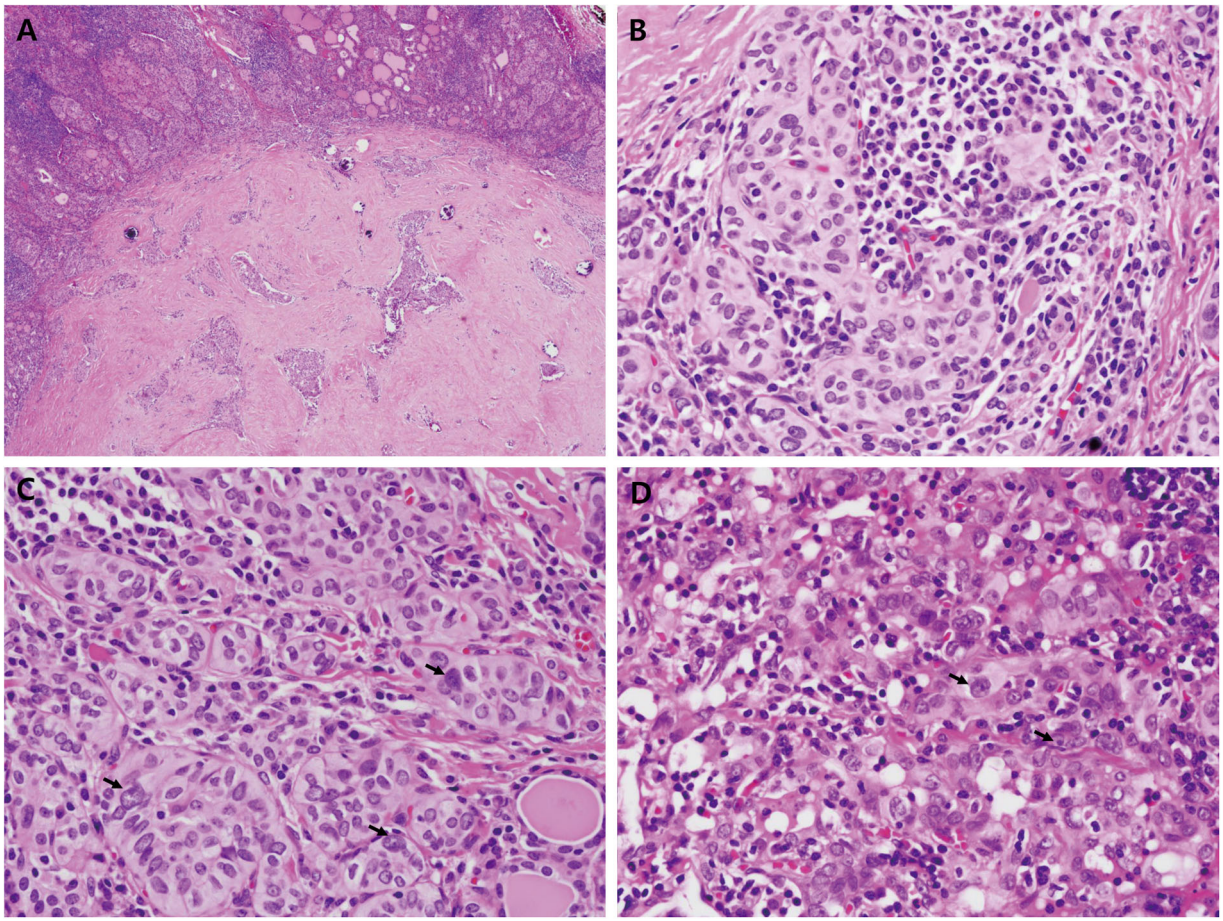

Fig. 3 Microscopic features of PTMC with *ALK* rearrangement in both PTMC and its metastatic LN. **a** A 0.8 cm sized ill-defined nodule reveals sclerotic stroma and numerous psammoma bodies in the background of lymphocytic thyroiditis. **b** Tumor cells show solid growth pattern, abundant cytoplasm, and heavy infiltration of plasma cells. **c**, **d** On high-power field, markedly enlarged nuclei (arrows) and anisokaryosis are occasionally observed in both PTMC **c** and metastatic LN **d**

their LN metastasis of differentiated thyroid cancer is high [17]. These findings suggest a minor role for genetic alterations in the process of LN metastases in PTMC. Morphological features, epigenetic changes, or a certain tumor microenvironment might affect the process of LN metastasis. In previous studies, PTCs with an invasive growth pattern or a higher density of tumor-associated macrophages were associated with the development of LN metastasis [17–20].

The *BRAF* V600E mutation was most commonly detected, and the prevalence was 72% in this study, which was significantly higher than the prevalence reported in a recent meta-analysis [5]. This high prevalence of the *BRAF* V600E mutation might be associated with the extensive LN metastasis or the aggressive characteristics of the PTMCs in this study. However, this high prevalence of *BRAF* V600E mutation also might be associated with the general higher prevalence of BRAF V600E mutation in PTCs from Korea and also might be skewed due to small number of patients [21].

RET rearrangements, the most frequent fusion in a previous The Cancer Genome Atlas (TCGA) analysis of PTC, and *ALK* rearrangements are known as oncogenic drivers of PTC and were mutually exclusive with the *BRAF* mutation [15]. In this study, we also found *RET* and *ALK* rearrangements in PTMCs, and those were also mutually exclusive with the *BRAF* mutation. In one patient, the *BRAF* mutation was detected in the primary tumor and only a *CCDC6/RET* rearrangement was detected in a metastatic LN. Because this patient had multifocal PTMCs, we thought that this metastatic LN might be originated from other primary tumor foci. Pathological characteristics of thyroid cancer with *ALK* rearrangement were not well elucidated. In this study, PTMC with *ALK* rearrangement showed solid growth pattern with plasma cell infiltration, which was consistent with the previous study [22]. The prevalence of *ALK* rearrangement in PTC is about 2.2% and is associated with young, female patients. ALK IHC is usually positive but it was negative in this case [23].

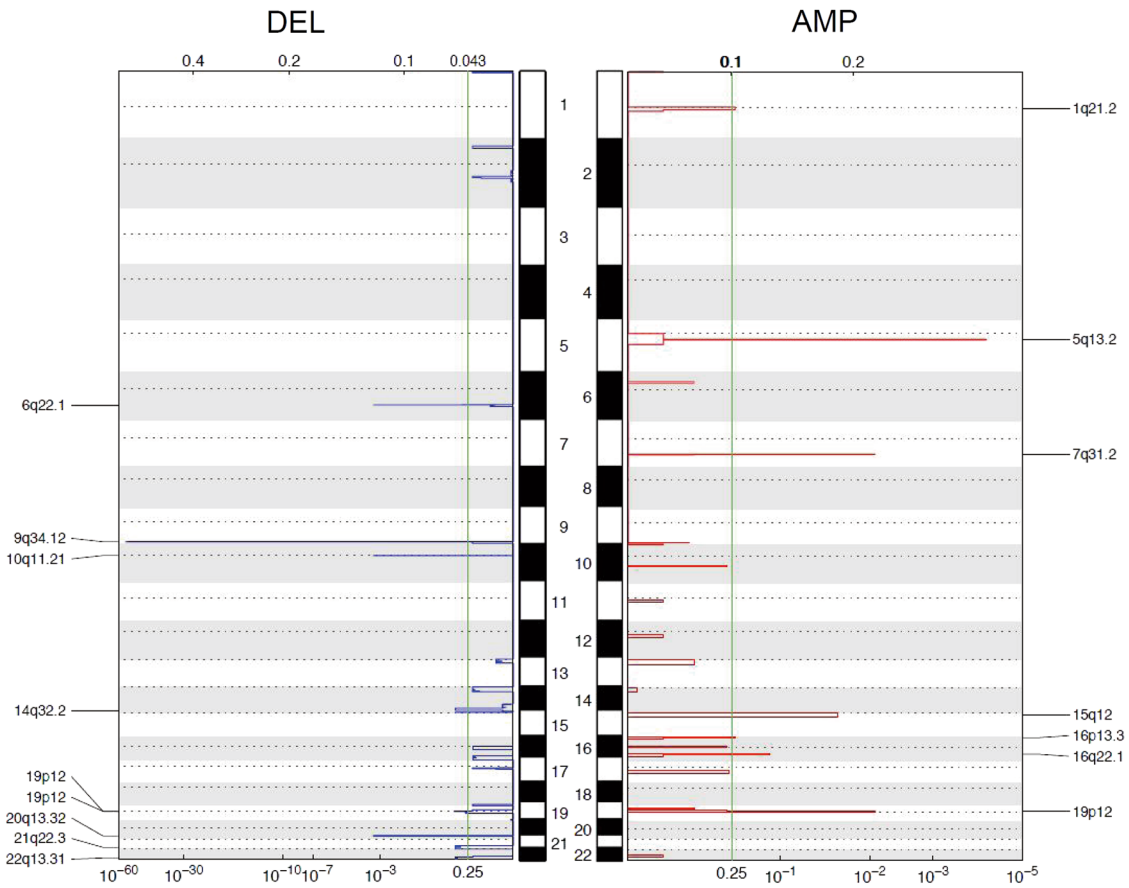

Fig. 4 Copy number variations (CNVs) in papillary thyroid microcarcinoma and its metastatic lymph node. Somatic CNV data for focal amplifications and deletions of 16 PTMC patients were analyzed using GISTIC2.0. The genome is oriented vertically from top to bottom, and the GISTIC *q*-values at each locus are plotted on a log scale from left to right. The green line represents the significance threshold (*q*-value = 0.25). DEL deletion, AMP amplification

Following the *BRAF* mutation, an in-frame deletion in *ACVR2A* and a nonsense mutation in *AR* were the prevalent somatic mutations in this study. Activin is a member of the transforming growth factor-beta superfamily, which shows the growth suppression effects, and inactivating mutations in *ACVR2A* have been reported in colon cancer, especially with high-frequency microsatellite instability [24, 25]. According to TCGA data for PTC, a missense mutation in *ACVR2A* has been detected in one sample among 482 samples, and the role of the inactivating mutation in *ACVR2A* has not been elucidated in thyroid cancers [22, 23]. The *AR* mutation has been most studied in prostate cancers and plays a significant role in prostate cancer progression [26]. As the prevalence and the prognosis of thyroid cancer are different between men and women, the expression of the estrogen receptor or AR has been reported for thyroid cancer. In one previous study, AR was expressed in about 20% of differentiated thyroid cancers, detected by immunohistochemistry in both men and women, and was associated with capsular invasion of the tumor [27]. However, an *AR* mutation has not been reported in thyroid cancer [22, 23].

We also analyzed somatic CNVs and found nine focal deletions and seven focal amplifications with GISTIC2 significance. Focal deletion of 9q was most common in our PTMC patients and has also been reported in a previous TCGA analysis of PTC [15]. A 22q deletion and 1q amplification have also been reported [15, 28]. However, we could not evaluate the association between the CNVs and the clinicopathological characteristics of PTMC patients because of the small number of patients.

Our study has limitations in that only a small number of PTMC patients were evaluated. We only evaluated the mutational profiles of PTMCs with extensive LN metastasis, and not those of the low-risk PTMCs in general. We could not evaluate the mutational profiles of distant metastatic tumors due to lack of tissues. We only evaluated the mutational profile of a dominant primary tumor. Furthermore, we only tested 382 known cancer-related genes by targeted sequencing. This might be the reason for the

inability to detect any genetic alterations in two of the PTMCs with metastatic LNs in this study. Furthermore, we could not evaluate *TERT* promoter mutation. Because of high GC content of *TERT* promoter, designing of good probes with high coverage for this region is impossible. However, the present study was the first comprehensive analysis of the mutational profile of PTMC, and we excluded germline changes by comparing the results for PTMC or the metastatic LN with those of matched normal tissues.

In conclusion, the mutational frequency of PTMCs was really low, even of those with extensive LN metastasis. The mutational status of the primary tumor and the metastatic LNs was not significantly different, and the *BRAF* V600E mutation was the most frequently mutated gene in both the primary and metastatic LNs. These findings suggest a minor role for genetic alterations in the process of LN metastasis in PTMC.

Funding This study was supported by the National Research Foundation (NRF) of Korea Research Grant (NRF-2017R1D1A1B03028231).

Compliance with ethical standards

Conflict of interest The authors declare that they have no conflict of interest.

Ethical approval All procedures performed in this study were in accordance with the ethical standards of the institutional review board and with the 1964 Helsinki declaration and its later amendments or comparable ethical standards.

Informed consent Informed consent was obtained from all participants included in the study, except 2two patients who died before the initiation of this study.

References

1. B.R. Haugen, E.K. Alexander, K.C. Bible, G.M. Doherty, S.J. Mandel, Y.E. Nikiforov, F. Pacini, G.W. Randolph, A.M. Sawka, M. Schlumberger, K.G. Schuff, S.I. Sherman, J.A. Sosa, D.L. Steward, R.M. Tuttle, L. Wartofsky, 2015 American Thyroid Association Management guidelines for adult patients with thyroid nodules and differentiated thyroid cancer: The American Thyroid Association Guidelines Task Force on Thyroid Nodules and Differentiated Thyroid Cancer. Thyroid **26**(1), 1–133 (2016). https://doi.org/10.1089/thy.2015.0020
2. H. Kwon, H.S. Oh, M. Kim, S. Park, M.J. Jeon, W.G. Kim, W.B. Kim, Y.K. Shong, D.E. Song, J.H. Baek, K.W. Chung, T.Y. Kim, Active surveillance for patients with papillary thyroid microcarcinoma: a single center's experience in Korea. J. Clin. Endocrinol. Metab. **102**(6), 1917–1925 (2017). https://doi.org/10.1210/jc.2016-4026
3. M.J. Jeon, W.G. Kim, Y.M. Choi, H. Kwon, Y.M. Lee, T.Y. Sung, J.H. Yoon, K.W. Chung, S.J. Hong, T.Y. Kim, Y.K. Shong, D.E. Song, W.B. Kim, Features predictive of distant metastasis in papillary thyroid microcarcinomas. Thyroid **26**(1), 161–168 (2016). https://doi.org/10.1089/thy.2015.0375
4. D. Li, M. Gao, X. Li, M. Xing, Molecular aberrance in papillary thyroid microcarcinoma bearing high aggressiveness: identifying a "Tibetan Mastiff dog" from puppies. J. Cell. Biochem. **117**(7), 1491–1496 (2016). https://doi.org/10.1002/jcb.25506
5. F. Li, G. Chen, C. Sheng, A.M. Gusdon, Y. Huang, Z. Lv, H. Xu, M. Xing, S. Qu, BRAFV600E mutation in papillary thyroid microcarcinoma: a meta-analysis. Endocr. Relat. Cancer **22**(2), 159–168 (2015). https://doi.org/10.1530/erc-14-0531
6. D. de Biase, G. Gandolfi, M. Ragazzi, M. Eszlinger, V. Sancisi, M. Gugnoni, M. Visani, A. Pession, G. Casadei, C. Durante, G. Costante, R. Bruno, M. Torlontano, R. Paschke, S. Filetti, S. Piana, A. Frasoldati, G. Tallini, A. Ciarrocchi, TERT promoter mutations in papillary thyroid microcarcinomas. Thyroid **25**(9), 1013–1019 (2015). https://doi.org/10.1089/thy.2015.0101
7. M.J. Jeon, S.M. Chun, D. Kim, H. Kwon, E.K. Jang, T.Y. Kim, W.B. Kim, Y.K. Shong, S.J. Jang, D.E. Song, W.G. Kim, Genomic alterations of anaplastic thyroid carcinoma detected by targeted massive parallel sequencing in a BRAF(V600E) mutation-prevalent area. Thyroid **26**(5), 683–690 (2016). https://doi.org/10.1089/thy.2015.0506
8. H. Li, R. Durbin, Fast and accurate short read alignment with Burrows-Wheeler transform. Bioinformatics **25**(14), 1754–1760 (2009). https://doi.org/10.1093/bioinformatics/btp324
9. A. McKenna, M. Hanna, E. Banks, A. Sivachenko, K. Cibulskis, A. Kernytsky, K. Garimella, D. Altshuler, S. Gabriel, M. Daly, M.A. DePristo, The Genome Analysis Toolkit: a MapReduce framework for analyzing next-generation DNA sequencing data. Genome Res. **20**(9), 1297–1303 (2010). https://doi.org/10.1101/gr.107524.110
10. K. Cibulskis, M.S. Lawrence, S.L. Carter, A. Sivachenko, D. Jaffe, C. Sougnez, S. Gabriel, M. Meyerson, E.S. Lander, G. Getz, Sensitive detection of somatic point mutations in impure and heterogeneous cancer samples. Nat. Biotechnol. **31**(3), 213–219 (2013). https://doi.org/10.1038/nbt.2514
11. E. Talevich, A.H. Shain, T. Botton, B.C. Bastian, CNVkit: genome-wide copy number detection and visualization from targeted DNA sequencing. PLoS Comput. Biol. **12**(4), e1004873 2016). https://doi.org/10.1371/journal.pcbi.1004873
12. R.P. Abo, M. Ducar, E.P. Garcia, A.R. Thorner, V. Rojas-Rudilla, L. Lin, L.M. Sholl, W.C. Hahn, M. Meyerson, N.I. Lindeman, P. Van Hummelen, L.E. MacConaill, BreaKmer: detection of structural variation in targeted massively parallel sequencing data using kmers. Nucleic Acids Res. **43**(3), e19 2015). https://doi.org/10.1093/nar/gku1211
13. C.H. Mermel, S.E. Schumacher, B. Hill, M.L. Meyerson, R. Beroukhim, G. Getz, GISTIC2.0 facilitates sensitive and confident localization of the targets of focal somatic copy-number alteration in human cancers. Genome Biol. **12**(4), R41 (2011). https://doi.org/10.1186/gb-2011-12-4-r41
14. M.B. Amin, S. Edge, F. Greene, D.R. Byrd, R.K. Brookland, M. K. Washington, J.E. Gershenwald, C.C. Compton, K.R. Hess, D. C. Sullivan, J.M. Jessup, J.D. Brierley, L.E. Gaspar, R.L. Schilsky, C.M. Balch, D.P. Winchester, E.A. Asare, M. Madera, D.M. Gress, L.R. Meyer, *AJCC Cancer Staging Manual*, 8th edn (Springer, New York, 2017)
15. T.C.G.A.R. Network, Integrated genomic characterization of papillary thyroid carcinoma. Cell **159**(3), 676–690 (2014). https://doi.org/10.1016/j.cell.2014.09.050
16. L.B. Alexandrov, S. Nik-Zainal, D.C. Wedge, S.A. Aparicio, S. Behjati, A.V. Biankin, G.R. Bignell, N. Bolli, A. Borg, A.L. Borresen-Dale, S. Boyault, B. Burkhardt, A.P. Butler, C. Caldas, H.R. Davies, C. Desmedt, R. Eils, J.E. Eyfjord, J.A. Foekens, M. Greaves, F. Hosoda, B. Hutter, T. Ilicic, S. Imbeaud, M. Imielinski, N. Jager, D.T. Jones, D. Jones, S. Knappskog, M. Kool, S.

R. Lakhani, C. Lopez-Otin, S. Martin, N.C. Munshi, H. Nakamura, P.A. Northcott, M. Pajic, E. Papaemmanuil, A. Paradiso, J. V. Pearson, X.S. Puente, K. Raine, M. Ramakrishna, A.L. Richardson, J. Richter, P. Rosenstiel, M. Schlesner, T.N. Schumacher, P.N. Span, J.W. Teague, Y. Totoki, A.N. Tutt, R. Valdes-Mas, M.M. van Buuren, L. van 't Veer, A. Vincent-Salomon, N. Waddell, L.R. Yates, J. Zucman-Rossi, P.A. Futreal, U. McDermott, P. Lichter, M. Meyerson, S.M. Grimmond, R. Siebert, E. Campo, T. Shibata, S.M. Pfister, P.J. Campbell, M.R. Stratton, Signatures of mutational processes in human cancer. Nature **500** (7463), 415–421 (2013). https://doi.org/10.1038/nature12477

17. M. Melo, A. Gaspar da Rocha, R. Batista, J. Vinagre, M.J. Martins, G. Costa, C. Ribeiro, F. Carrilho, V. Leite, C. Lobo, J.M. Cameselle-Teijeiro, B. Cavadas, L. Pereira, M. Sobrinho-Simoes, P. Soares, TERT, BRAF, and NRAS in primary thyroid cancer and metastatic disease. J. Clin. Endocrinol. Metab. **102**(6), 1898–1907 (2017). https://doi.org/10.1210/jc.2016-2785
18. K.T. Huynh, D.S. Hoon, Epigenetics of regional lymph node metastasis in solid tumors. Clin. Exp. Metastasis **29**(7), 747–756 (2012). https://doi.org/10.1007/s10585-012-9491-3
19. C. Eloy, J. Santos, P. Soares, M. Sobrinho-Simoes, The preeminence of growth pattern and invasiveness and the limited influence of BRAF and RAS mutations in the occurrence of papillary thyroid carcinoma lymph node metastases. Virchows Arch. **459**(3), 265–276 (2011). https://doi.org/10.1007/s00428-011-1133-7
20. W. Qing, W.Y. Fang, L. Ye, L.Y. Shen, X.F. Zhang, X.C. Fei, X. Chen, W.Q. Wang, X.Y. Li, J.C. Xiao, G. Ning, Density of tumor-associated macrophages correlates with lymph node metastasis in papillary thyroid carcinoma. Thyroid **22**(9), 905–910 (2012). https://doi.org/10.1089/thy.2011.0452
21. G. Gandolfi, V. Sancisi, S. Piana, A. Ciarrocchi, Time to reconsider the meaning of BRAF V600E mutation in papillary thyroid carcinoma. Int. J. Cancer **137**(5), 1001–1011 (2015). https://doi.org/10.1002/ijc.28976
22. A. Chou, S. Fraser, C.W. Toon, A. Clarkson, L. Sioson, M. Farzin, C. Cussigh, A. Aniss, C. O'Neill, N. Watson, R.J. Clifton-Bligh, D.L. Learoyd, B.G. Robinson, C.I. Selinger, L.W. Delbridge, S.B. Sidhu, S.A. O'Toole, M. Sywak, A.J. Gill, A detailed clinicopathologic study of ALK-translocated papillary thyroid carcinoma. Am. J. Surg. Pathol. **39**(5), 652–659 (2015). https://doi.org/10.1097/pas.0000000000000368
23. G. Perot, I. Soubeyran, A. Ribeiro, B. Bonhomme, F. Savagner, N. Boutet-Bouzamondo, I. Hostein, F. Bonichon, Y. Godbert, F. Chibon, Identification of a recurrent STRN/ALK fusion in thyroid carcinomas. PLoS ONE **9**(1), e87170 (2014). https://doi.org/10.1371/journal.pone.0087170
24. J. Bauer, O. Ozden, N. Akagi, T. Carroll, D.R. Principe, J.J. Staudacher, M.E. Spehlmann, L. Eckmann, P.J. Grippo, B. Jung, Activin and TGFbeta use diverging mitogenic signaling in advanced colon cancer. Mol. Cancer **14**, 182 (2015). https://doi.org/10.1186/s12943-015-0456-4
25. R.J. Hause, C.C. Pritchard, J. Shendure, S.J. Salipante, Classification and characterization of microsatellite instability across 18 cancer types. Nat. Med. **22**(11), 1342–1350 (2016). https://doi.org/10.1038/nm.4191
26. Z. Culig, F.R. Santer, Androgen receptor signaling in prostate cancer. Cancer Metastasis Rev. **33**(2–3), 413–427 (2014). https://doi.org/10.1007/s10555-013-9474-0
27. F. Magri, V. Capelli, M. Rotondi, P. Leporati, L. La Manna, R. Ruggiero, A. Malovini, R. Bellazzi, L. Villani, L. Chiovato, Expression of estrogen and androgen receptors in differentiated thyroid cancer: an additional criterion to assess the patient's risk. Endocr. Relat. Cancer **19**(4), 463–471 (2012). https://doi.org/10.1530/erc-11-0389
28. G. Gandolfi, M. Ragazzi, D. de Biase, M. Visani, E. Zanetti, F. Torricelli, V. Sancisi, M. Gugnoni, G. Manzotti, L. Braglia, S. Cavuto, D.F. Merlo, G. Tallini, A. Frasoldati, S. Piana, A. Ciarrocchi, Genome-wide profiling identifies the THYT1 signature as a distinctive feature of widely metastatic papillary thyroid carcinomas. Oncotarget **9**(2), 1813–1825 (2018). https://doi.org/10.18632/oncotarget.22805